Received: 10 May 2019 | Revised: 12 August 2019 | Accepted: 23 September 2019

DOI: 10.1002/suco.201900176

TECHNICAL PAPER

fib WILEY

Punching behavior of BubbleDeck type reinforced concrete slabs

Wanderley G. Nicácio[1] | **Joaquim A. O. Barros**[2] | **Guilherme S. S. A. Melo**[1]

[1]Faculty of Technology, Department of Civil Engineering, University of Brasilia-UnB, Brasília, Brazil

[2]Department of Civil Engineering, ISISE, Institute of Science and Innovation for Bio-Sustainability (IB-S), University of Minho, Guimarães, Portugal

Correspondence
Joaquim Barros, Department of Civil Engineering, ISISE, Institute of Science and Innovation for Bio-Sustainability (IB-S), University of Minho, Guimarães, Portugal.
Email: barros@civil.uminho.pt

Funding information
CAPES, Grant/Award Number: PDSE program/Process number 88881.134825/2016-01; FCT, Grant/Award Number: project ICoSyTec POCI-01-0145-FEDER-027990

Abstract

The BubbleDeck type slab (BD) is a reinforced concrete (RC) flat slab that includes recycled plastic hollow spheres (RPHS) in its core for decreasing its dead weight. However, punching capacity of BD slabs can be a critical aspect, thereby this work is devoted to assess experimentally its punching behavior. An experimental program composed of four real scale prototypes, representative of RC flat slabs in punching loading conditions, was carried out. Two of these slabs are of BD type, while the other two do not include the RPHS system, herein denominated as RC solid slab (SS). The test results show that all the tested slabs failed in punching after the occurrence of yield initiation of the flexural reinforcement. The punching capacity and the deflection at failure of BD type slab has decreased up to 14% and up to 44%, respectively, when compared to the corresponding SS type slab. A relatively small ductility index was obtained (between 1.51 and 2.65). In BD type slabs, the punching failure surface had tendency to propagate through the RPHS, at an inclination angle of about 45°.

KEYWORDS

BubbleDeck type slabs, finite element method, material nonlinear analysis, punching, reinforced concrete flat slabs

1 | INTRODUCTION

Several strategies are being used for decreasing the deadweight of reinforced concrete (RC) slabs, since significant economy can be obtained in the slab and in direct and indirect supporting elements, such is the case of columns, foundations, and shear walls.

In the 1990s of the 20th century, a new type of lightweight RC slab has started being used that includes a core formed by recycled plastic hollow spheres (RPHS), whose spacing and positioning are ensured by the help of a top and bottom steel meshes, as shown in Figure 1a. This type of slab is denominated as *BubbleDeck*, hereafter abbreviated by the acronym BD. For speeding up the construction process of BD type RC slabs, precast floor plates can be adopted (Figure 1b), serving as permanent molds, which introduce an interface between this plate and the concrete cast in place, whose consequences for the load carrying capacity of the BD slab should be assessed. These precast floor plates can decrease significantly the material resources, time, and costs related to the formwork and scaffold systems of the BD slabs. This type of slab, herein designated by the acronym BDP, is also investigated in the present work. A third methodology of producing BD type slabs is represented in Figure 1c, where finished panels are supplied, and the continuity between consecutive panels is ensured by the superposition of the flexural reinforcement and concrete casting in place of these connection zones.

Experimental tests with BD type RC slabs have demonstrated that their flexural stiffness, compared to those where concrete occupy the space of RPHS (solid RC slabs, herein abbreviated by the acronym of SS), is in the interval of

Discussion on this paper must be submitted within two months of the print publication. The discussion will then be published in print, along with the authors' closure, if any, approximately nine months after the print publication.

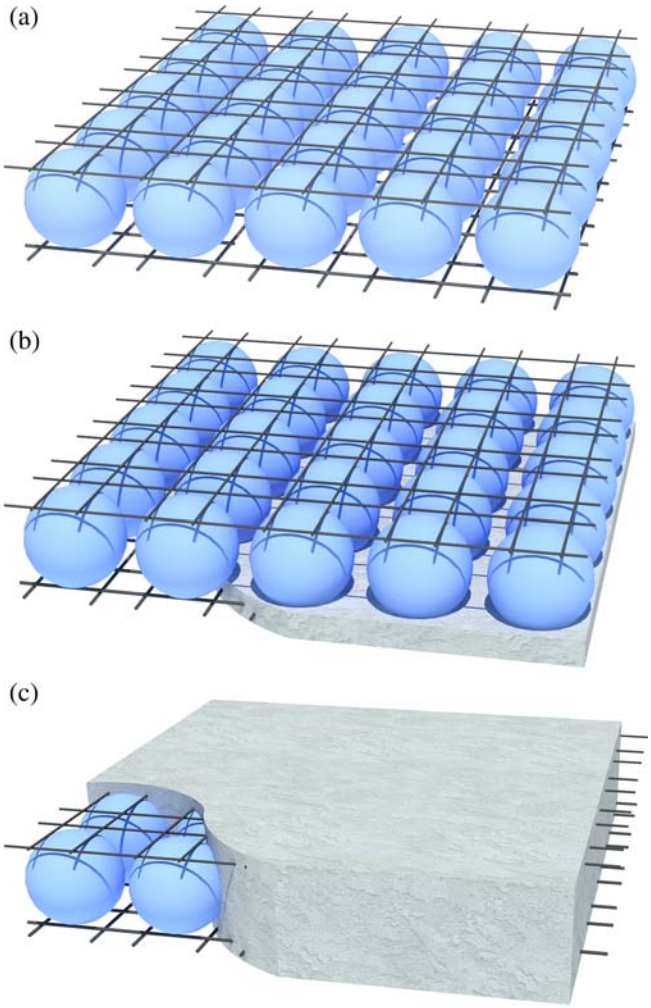

FIGURE 1 *BubbleDeck* type RC flat slab (BD): (a) lightweight system formed by RPHS in-between steel meshes, (b) lightweight system including a bottom RC concrete layer, (c) prefabricated modules of BD. RC, reinforced concrete; RPHS, recycled plastic hollow spheres

87–93%, having been recommended the value of 90%.[1,2] For the cracking, bending moment is suggested 80% of the one of corresponding SS slab.[1]

The displacement ductility performance of BD slabs was investigated by numerical simulations, where ductility index ($\mu = \delta_p/\delta_y$) was defined as the ratio between deflection at failure (δ_p) and deflection and yield initiation of the flexural reinforcement (δ_y). According to these studies, a ductility performance $\mu > 3$ was recommended for BD slabs.[3]

Some theoretical and experimental research have also suggested the BD RC slabs can be regarded, from the design point of view, as solid RC slabs, but the available recommendations are of empirical nature, and are based on very few experimental results, consisting as reducing the punching capacity of the corresponding solid RC slab in a factor that is around 40%.[4,5] Therefore, reliable information is still scarce for assessing the level of "appropriateness" of the suggested recommendations.

The BD is classified as a flat RC slab, which is directly supported on the columns. This has several technical advantages when compared to RC slabs supported on beams, namely: formworks of simpler geometry and faster to be assembled and disassembled; quicker construction process; the restrictions on changing the layout of compartment configurations, imposed by the presence of the beams in the RC slabs supported on beams, do not exist in BD slabs; reduction of the total height of a building for the same occupancy area. These technical advantages increase the cost competitiveness of the BD solutions.

In spite of these advantages, attributed to the BD type RC slabs, their use is still very moderate, which might be caused by the design concerns about their punching capacity due to the presence of RPHS. Punching failure mode is generally catastrophic and can cause the global collapse of a building,[6] therefore, a construction system susceptible to this type of failure mode must be designed by a comprehensive approach, whose predictive performance must have been validated from experimental tests.

In floor plates with void formers, a certain area around their vertical structural supports does not include lightweight components in order to guarantee the required punching capacity. In research context, some authors have limited this solid concrete area to a cross type configuration, by also using shear reinforcement in these concrete solid zones.[7] By testing lightweight type slabs with this concrete solid cross type configuration, as well as slabs with lightweight components in their total area, they verified that the first type of slabs has presented a punching capacity 18% higher than the one registered in the second type slab.[7]

Held and Pfeffer[4] tested six BD slabs without solid concrete zones around the vertical supporting elements and without punching reinforcement. This experimental program was composed by two series of three slab prototypes, one with slab's dimensions of $2{,}500 \times 2{,}500 \times 240$ mm^3, and the other of $2{,}500 \times 2{,}500 \times 450$ mm^3, made by concrete of average compressive strength of 30 and 40 MPa, respectively. The authors verified that BD RC slabs presented a punching capacity 62% of the corresponding concrete solid RC slabs. Available design recommendations are suggesting 60% for this ratio.[5] These design recommendations are supported on the formulations already existing for conventional solid type RC slabs, where the decrease of concrete resisting punching surface, due to the presence of the lightweight components, is taken into account. By applying this approach, good estimates of the punching capacity registered in experimental tests were obtained,[4] but its full acceptance requires to be applied to a comprehensive set of experimental tests, of statistical relevance, carried out with representative

prototypes and loading conditions. Other experimental tests with BD RC slabs have demonstrated that using steel girders in the solid zones between lightweight components (disposed in only one direction of the slab's orthotropy) has increased the punching capacity in 30% regarding the corresponding BD RC slabs without this type of reinforcement.[8]

The punching capacity of a RC slab can also be increased by using specific reinforcement,[9–11] concrete of higher

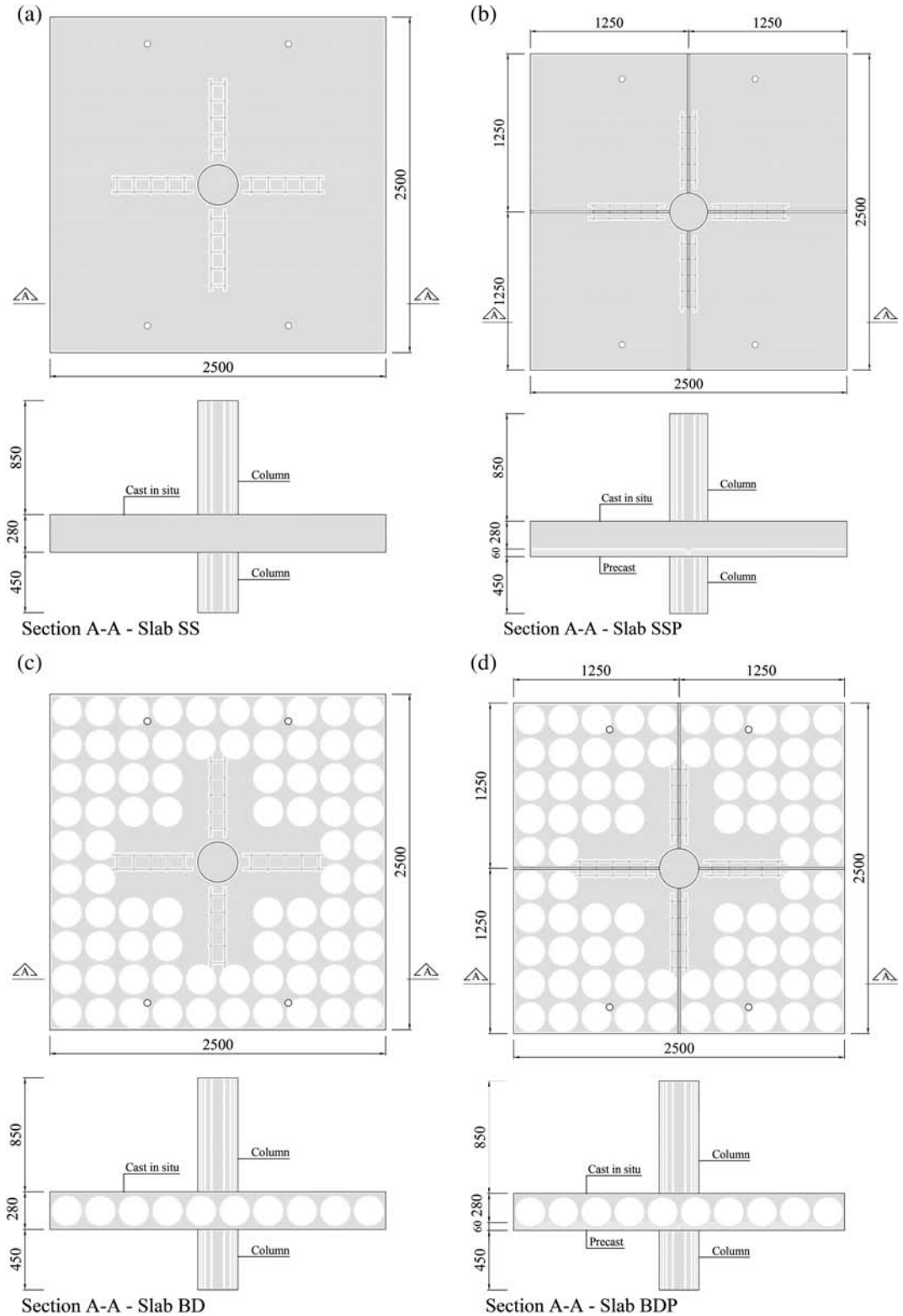

FIGURE 2 Geometry of the slab's prototype: (a) SS, (b) SSP, (c) BD, and (d) BDP (dimensions in mm). BD, *BubbleDeck* slab; SS, solid slab

strength class,[12] fiber reinforcement,[12,13] and enlarging the cross section of the supporting vertical elements in order to promote the development of punching failure surfaces of larger area.[14]

The existing research on the BD type RC slabs with RPHS is basically dedicated to their flexural and shear capacity assessed in one-way prototypes (working like shallow beams), which is not representative of slabs supported on columns.[2,15–17]

The present work aims to investigate experimentally the behavior of real scale BD type RC prototypes tested in conditions where only axial load is transferred from the slab to the supporting column. These conditions are representative of slabs supported on internal columns of building structural systems. For assessing the punching performance of BD type RC slabs, solid type RC slabs were also tested and the results are compared.

2 | EXPERIMENTAL PROGRAM

2.1 | Geometry and reinforcement arrangements of the prototypes

The experimental program is composed of the four slabs shown in Figure 2: two of *BubbleDeck* slab (BD and BDP, Figure 2c,d, respectively) and the other two, serving as reference specimens, where the unique difference for the corresponding BD is resumed to the substitution of the RPHS by concrete (SS and SSP, Figure 2a,b, respectively), for example, these are solid RC slabs. The differences between the slabs in each of these two groups are restricted to the adoption of a precast RC floor plate positioned in the compression zone of the slab, which also introduces alterations on the anchorage conditions of the punching reinforcement. The other slab in each group is integrally cast in situ. In real practice, this precast RC floor plate (in general is a prefabricated RC panel) is an option for speeding up the construction process of this type of slabs.

All the slab prototypes have dimensions of 2,500 × 2,500 × 280 mm^3, and in each slab's center exists a circular RC column of 300 mm diameter, and 850 and 450 mm length above and below of the slab, respectively (Figure 2). The RPHS are of high-density polyethylene, of 225 mm diameter and spaced at 250 mm in both directions of the slab, measured between the centers of consecutive RPHS. The slabs SS and BD, represented in Figure 2a,c, respectively, were fully cast in one phase, while SSP and BDP, shown in Figure 2b, d, respectively, were executed in the following three phases: a first phase where the four precast RC floor plates, with the geometry shown in Figure 3, are cast; a second phase dedicated to the placement of the system composed

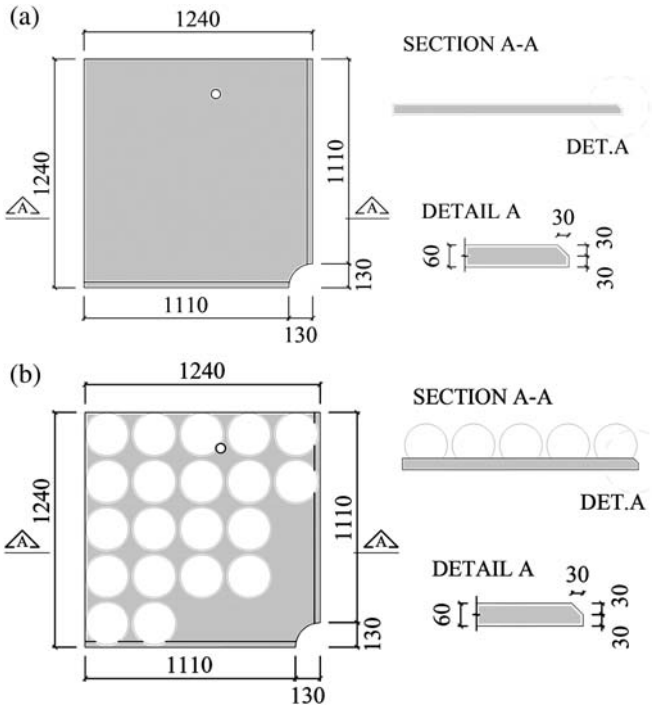

FIGURE 3 Geometry of the precast layer used in slab: (a) SSP, (b) BDP (dimensions in mm). BDP, *BubbleDeck* slab with precast floor plates; SSP, solid slab with precast floor plates

of the RPHS and its top steel mesh while the concrete of the precast RC floor plate is still fresh; the last phase is concerned to the concrete casting of the remaining volume of the slab. The sequence of the execution procedures of the slabs are shown in Figure 4.

The reinforcement details of the slabs of the experimental program are represented in Figure 5. A flexural reinforcement ratio (ρ_f) of 0.41% in both directions was adopted in the top part for all the slabs (the one to be in tension). In the BD slabs, the RPHS were maintained in their intended position by using a top and bottom steel mesh of 6 and 8 mm diameter bars of equal reinforcement ratio in both directions of, respectively, 0.10 and 0.12%.

This reinforcement was also applied in the SS slabs in order to have the same flexural reinforcement in all the slabs of the experimental program. In the SSP and BDP slabs, the aforementioned bottom steel mesh was adopted for the reinforcement of the precast RC floor plate. In these last two slabs, steel bars of 10 mm diameter, length of 750 mm, and spaced at 250 mm and with a nominal cover of 10 mm were disposed symmetrically and transversally to the joints of the precast concrete layers (Figures 4 and 6).

In the BD and BDP slabs, the steel girders shown in Figure 7 were used to keep the bubbles fixed between the top and bottom reinforcement and to lift and transport the precast floor plates. Available design recommendations suggest that their influence on structural behavior is negligible.[5]

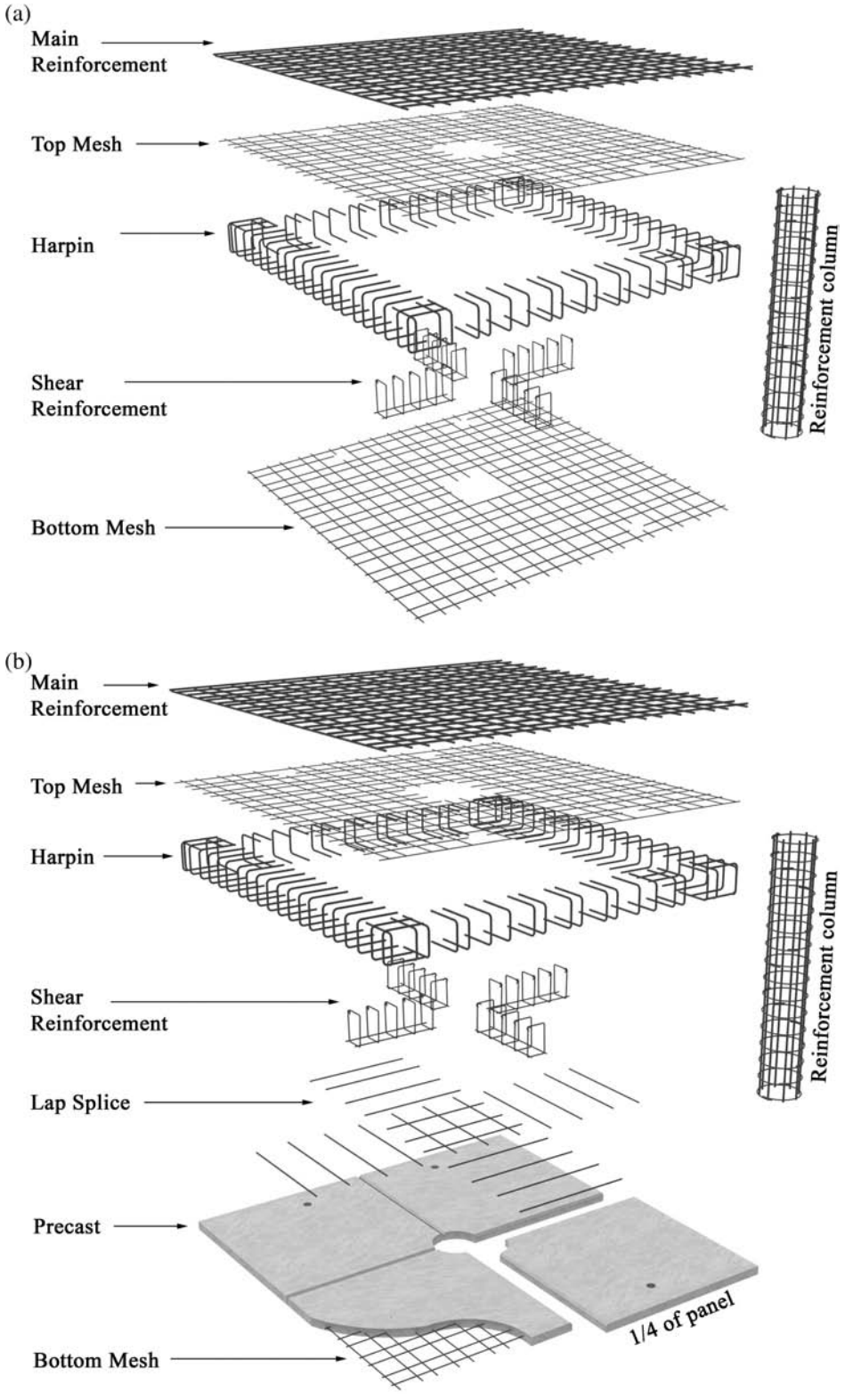

FIGURE 4 Schematic representation of the execution procedures of the slabs: (a) SS, (b) SSP, (c) BD, and (d) BDP (dimensions in mm). BD, *BubbleDeck* slab; SS, solid slab

For the punching reinforcement, 20 closed configuration steel stirrups of 8 mm diameter were disposed in a cross arrangement (Figure 8a) at a spacing of 125 mm, being the column's closest ones at 100 mm from the face of the column. In the SS and BD slabs, the steel stirrups embrace the top and bottom flexural reinforcement, while in the SSP and BDP they only involve the top flexural reinforcement and are supported on the top surface of the precast RC floor plate (Figure 8b).

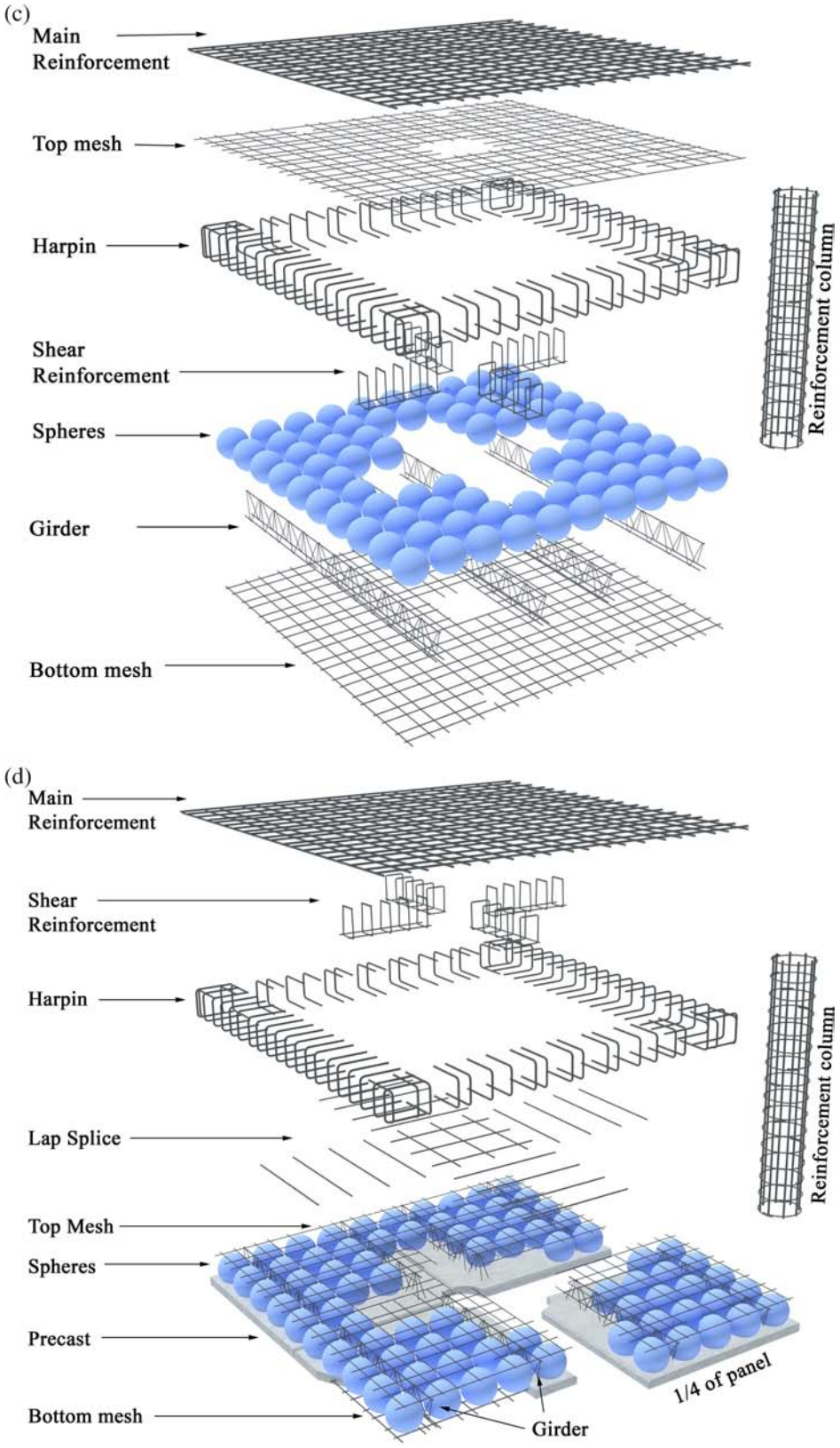

FIGURE 4 (Continued)

2.2 | Properties of the constituents materials

The concrete compressive strength (f_{cm}), splitting tensile strength ($f_{t,Dm}$), and Young's modulus (E_{cm}) were assessed by performing experimental tests in three cylindrical specimens of 100 mm diameter and 200 mm length (for each type of test), according to the recommendations of ABNT NBR 5739 (2007),[18] ABNT NBR 7222 (2011),[19] and ABNT NBR 8522 (2008)[20] standards, respectively. These tests were executed in the same day the corresponding slab prototypes were tested. The curing conditions of the materials and slab specimens followed the recommendations of ABNT NBR 5738 (2015)[21] and ABNT NBR 14931 (2004)[22] standards, respectively. The obtained average values and corresponding coefficient of variation (COV) for the concrete applied in the precast RC floor plates, SS and BD slabs are included in Table 1.

The properties of the steel reinforcements, namely the average values of the elasticity modulus (E_{sm}), yield stress (f_{ysm}), and corresponding strain (ε_{ysm}), were evaluated following the recommendations of ABNT NBR 6892 (2013),[23] by testing three specimens for each type of reinforcement. The obtained values and corresponding COV are indicated in Table 2.

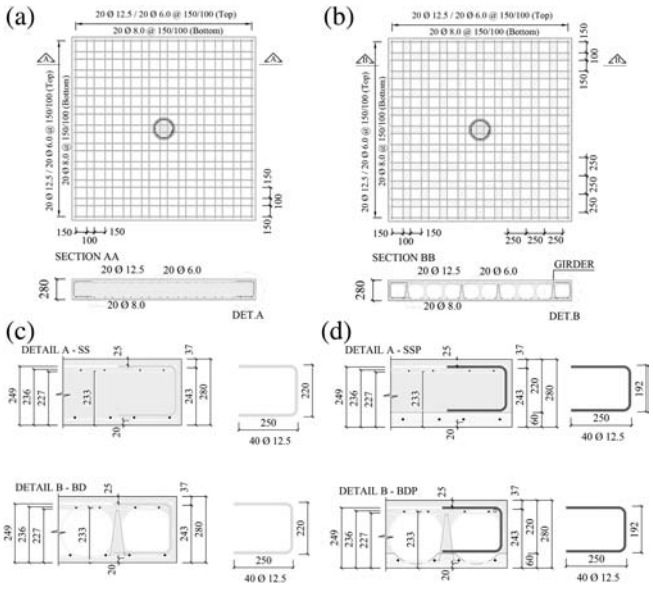

FIGURE 5 Reinforcements: (a) SS slab, (b) BD slab, (c) details in SS and BD slabs, (d) details in the SSP and BDP slabs (dimensions in mm). BD, *BubbleDeck* slab; SS, solid slab

2.3 | Test setup and monitoring system

The support and loading conditions of the tested slabs are represented in Figure 9. The loading was applied by using two sets of two hydraulic actuators, having each set been controlled by an independent hydraulic system. These four actuators apply a downward load in steel profiles that distributed the force in two zones of contact with the slab through a steel plate of $140 \times 140 \times 35$ mm^3 dimensions. Therefore, each slab was subjected to eight loading zones of contact area of 140×140 mm^2. The geometric center of each of these loading areas is at a radial distance of 981 mm from the external column's surface.

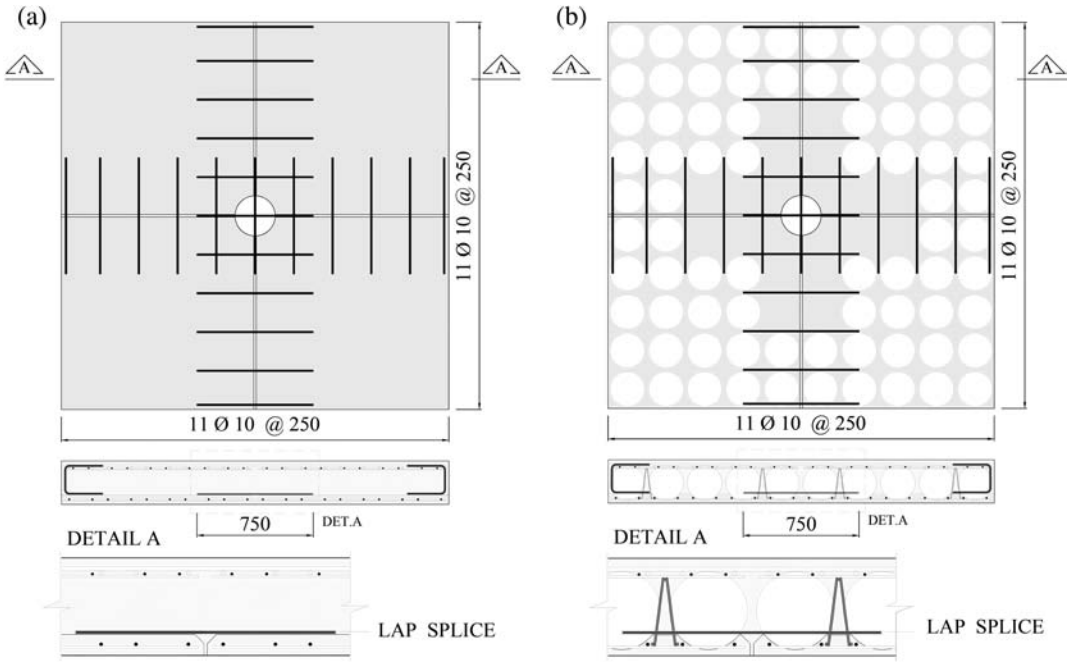

FIGURE 6 Details of the reinforcement on the joints between adjacent precast layers in the slab: (a) SSP, (b) BDP (dimensions in mm)

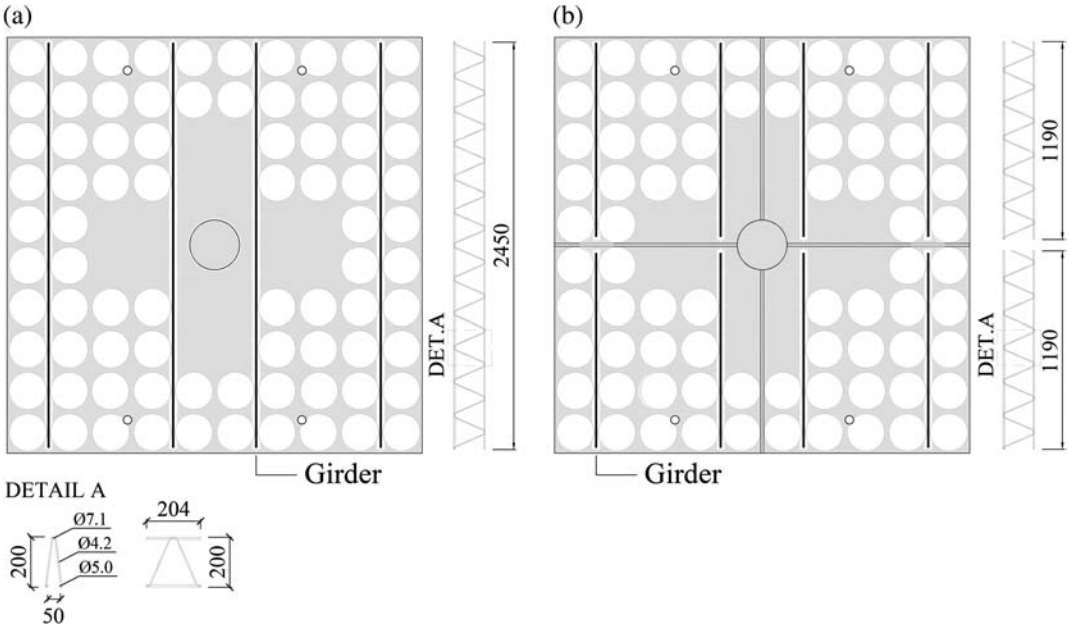

FIGURE 7 Disposition of the girders in slab: (a) *BubbleDeck* slab (BD), (b) BDP (dimensions in mm)

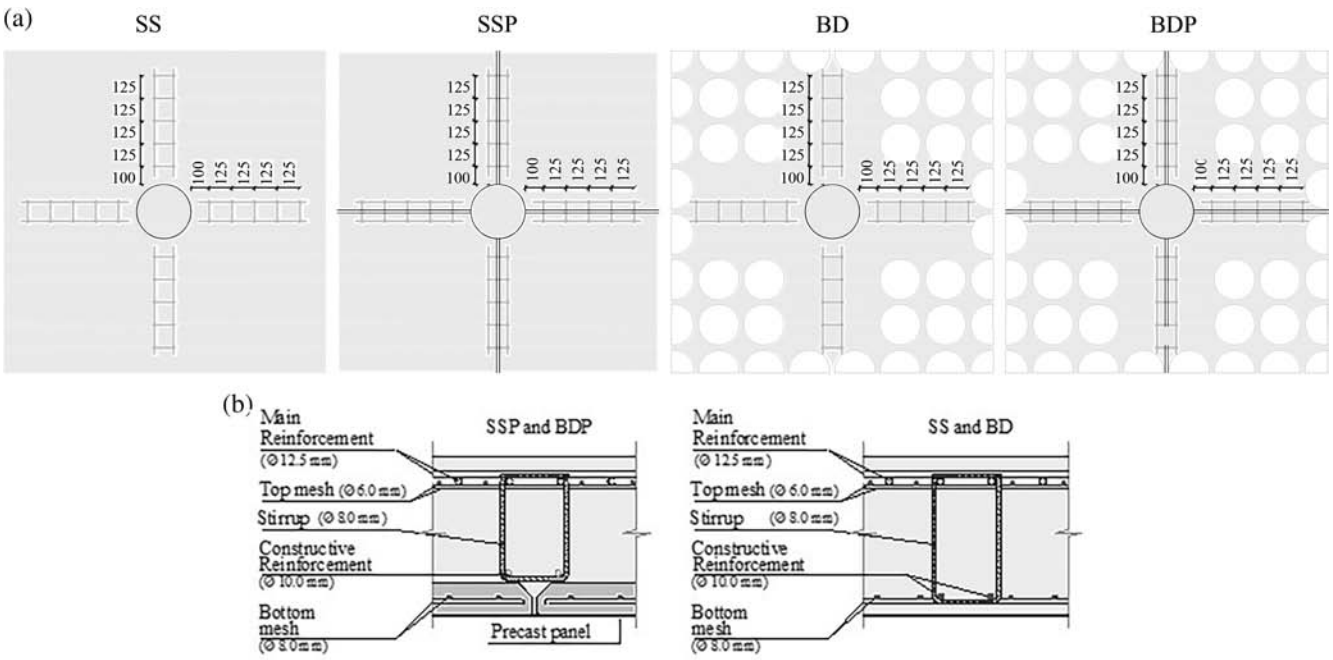

FIGURE 8 Details of the punching reinforcement: (a) plant view, (b) cross section (dimensions in mm)

TABLE 1 Concrete properties

Slab	f_{cm} (MPa)	COV (%)	$f_{t,Dm}$ (MPa)	COV (%)	E_{cm} (GPa)	COV (%)
Precast layer	34.9	5.7	3.6	5.3	28.3	8.5
SS and SSP	44.6	5.7	3.8	3.0	28.6	8.6
BD and BDP	47.0	9.1	3.0	8.1	28.6	13.9

Abbreviations: BD, *BubbleDeck* slab; SS, solid slab.

TABLE 2 Properties of the steel reinforcements (values in round brackets are COV)

	Type of reinforcement				
	Mesh Diameter (mm)		Bar Diameter (mm)		
Property	**6**	**8**	**8**	**10**	**12.5**
E_{sm} (GPa)	190 (4.1%)	194 (3%)	196 (3.5%)	193 (3.9%)	183 (2.8%)
f_{ysm} (MPa)	627 (0.7%)	681 (1.6%)	675 (6.8%)	618 (1.1%)	577 (0.2%)
ε_{ysm} (‰)	3.3 (4.6%)	3.5 (1.8%)	3.4 (3.3%)	3.2 (3.2%)	3.1 (3.0%)

Abbreviation: COV, coefficient of variation.

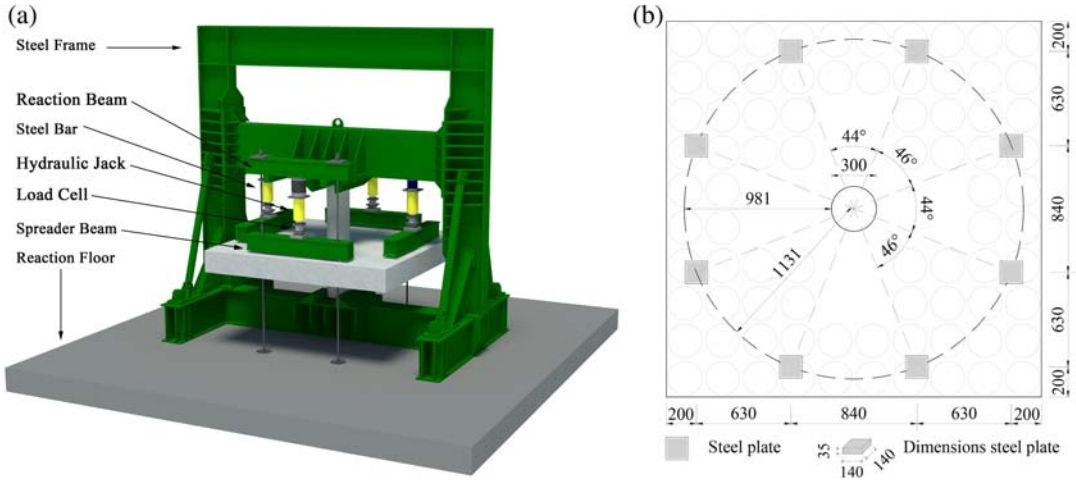

FIGURE 9 Test setup: (a) virtual representation, (b) location of the steel plates where the load was applied (dimensions in mm)

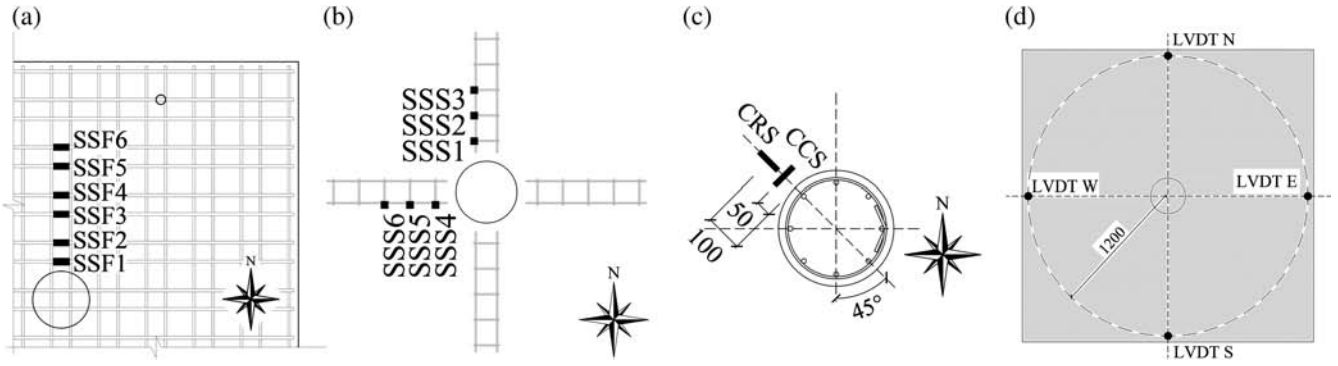

FIGURE 10 Monitoring system: Arrangement of strain gauges attached on the (a) top flexural reinforcement (that will be in tension), (b) stirrups, (c) slab's bottom concrete surface, (d) Arrangement of linear variable-displacement transducers (dimensions in mm)

The tests were conducted under force control with load increment of 20 kN up to 300 kN, followed of 40 kN up to the collapse of the slab. The monitoring of the applied load was performed by load cells individually aligned to each hydraulic actuator, ensuring uniform distribution of load on a test slab.

The strains in the top flexural reinforcement were registered by using six pairs of strain gauges disposed according to the schematic representation of Figure 10a (SSF1 to SSF6—each SSFi is composed of a pair of strain gauges applied in lateral sides diametrically opposed).

For measuring the strains in the punching reinforcement, strain gauges installed in the mid-depth of one of the vertical legs of the stirrups were applied according to the disposition shown in Figure 10b (SSS1–SSS6).

For measuring the strains in the concrete at the bottom surface of the slab, in the critical zone close to the column, two strain gauges were applied according to the configuration

TABLE 3 Load carrying capacity and deflection performance of the tested slabs

Slab	V_{max} (kN)	$\frac{V_{max}^{SSP(BDP)} - V_{max}^{SS(BD)}}{V_{max}^{SS(BD)}}$ (%)	$\frac{V_{max}^{BDi} - V_{max}^{SSi}}{V_{max}^{SSi}}$ (%)	$\delta_{V_{max}}$ (mm)	$\frac{\delta_{V_{max}}^{SSP(BDP)} - \delta_{V_{max}}^{SS(BD)}}{\delta_{V_{max}}^{SS(BD)}}$ (%)	$\frac{\delta_{V_{max}}^{BDi} - \delta_{V_{max}}^{SSi}}{\delta_{V_{max}}^{SSi}}$ (%)
SS	1,041	–	–	17.1	–	–
SSP	987	−5.2	–	22.4	31.0	–
BD	995	–	−4.4	15.8	–	−7.6
BDP	846	−15.0	−14.3	12.6	−20.3	−43.8

Abbreviations: BD, *BubbleDeck* slab; SS, solid slab.

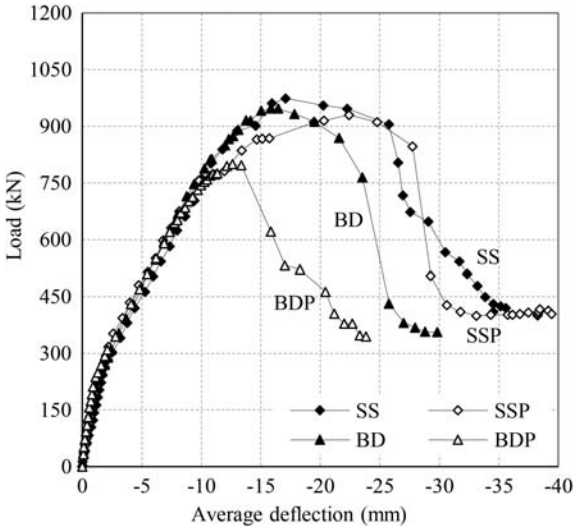

FIGURE 11 Load versus average deflection for the slabs of the experimental program

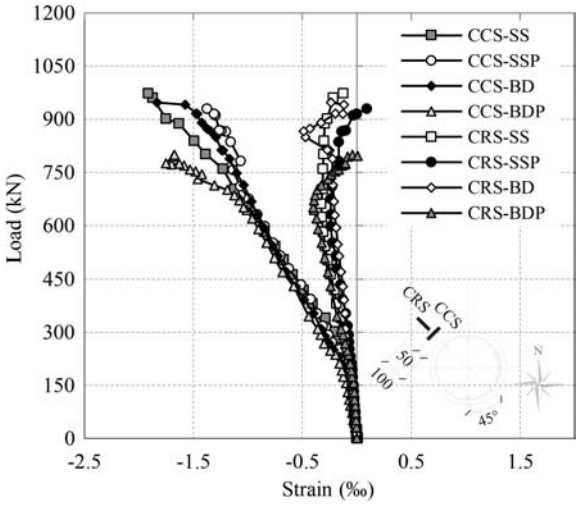

FIGURE 12 Load versus radial and circumferential strains in the concrete bottom slab's surface

represented in Figure 10c, where CRS intends to measure the Concrete Radial Strain, while CCS the Concrete Circumferential Strain. Four linear variable-displacement transducers (LVDT), whose disposition is shown in Figure 10d, supported on an external system to the testing reaction structure, were used for measuring the vertical deflection of the slab in the points where they were located.

3 | EXPERIMENTAL RESULTS AND DISCUSSION

3.1 | Load carrying and deflection capacities

The load carrying capacity and the deflection at peak load of the tested slabs are indicated in Table 3, while the load versus average deflection (average of the displacements measured by the LVDTs, Figure 10d) relationships are depicted in Figure 11. The parameter $\left(V_{max}^{SSP(BDP)} - V_{max}^{SS(BD)}\right)/V_{max}^{SS(BD)}$ aims to assess the influence of using the precast RC floor plates in the SSP and BDP series of slabs, where $V_{max}^{SSP(BDP)}$ and $V_{max}^{SS(BD)}$ are the load carrying capacity of the slab (SS and BD) with, and without, respectively, the precast RC floor plates. It is verified that using the precast RC floor plates has decreased the V_{max} in 5 and 15% in the series SS and BD, respectively. This is due to the casting discontinuity that caused a weakness at the interface between the precast RC floor plates and the remain concrete volume cast in a second stage (Figures 4, 6, and 8). The smaller vertical arms of the transverse reinforcement have also contributed for this effect since they were not so effectively anchored (Figure 8b). A similar decrease of load carrying capacity was registered in the BD slab when compared to the corresponding SS slab (−4.4 and −14.3% in the BD and BDP), which indicates that the resisting punching concrete surface has decreased due to the presence of the RPHS, despite their removal in the zone around the column, as shown in Figure 2. These reduction levels registered in the BD series are in agreement with the values obtained by other researcher.[4]

The average deflection at peak load was larger in the SS series, and no tendency was registered in terms of the influence of the precast RC floor plates for the slab's deformability.

Figure 11 shows that up to about ≈740 kN (and ≈10 mm deflection) the load versus average deflection was almost coincident in all the tested slabs, and the loss of stiffness

was mainly governed by the formation and propagation of flexural cracks. Above this deflection level, damage was intensified due to the formation of punching shear cracks, having the BD slabs presented smaller deflection capacity, but all the slabs experienced an abrupt load decay due to punching failure mode, with a residual load carrying capacity of about 415 and 350 kN in the series SS and BD, respectively.

3.2 | Concrete strains

Figure 10c shows the locations where the strain gauges were placed on the slab's bottom concrete surface for measuring the radial (CRS) and circumferential (CCS) strains. The relationship between the applied load and the strains registered in these strain gauges are presented in Figure 12. As expected, compressive radial and circumferential strains (negative values) were recorded up to almost the failure of the tested slabs. An inflection of the radial strain evolution was observed when damage, due to punching, started being localized, resulting even tensile radial strains at failure stage, which is in agreement with results registered by other authors in punching tests with flat RC slabs.[24,25] As shown in Figure 13, when this inflection occurred, the first two bars of the flexural reinforcement counted from the column's surface have already yielded.

Although the concrete radial strains had almost linearly increased up to the aforementioned inflection stage, the circumferential compressive strains had a significant increase after concrete crack initiation, with another increase of compressive strain gradient when flexural reinforcement started yielding. However, the maximum circumferential compressive strain was well below the concrete crushing strain, which is also an indication of punching failure occurrence.

3.3 | Strains in the flexural and punching reinforcement

Figure 10a shows the location and the designation of the strain gauges adopted for measuring strain evolution on the

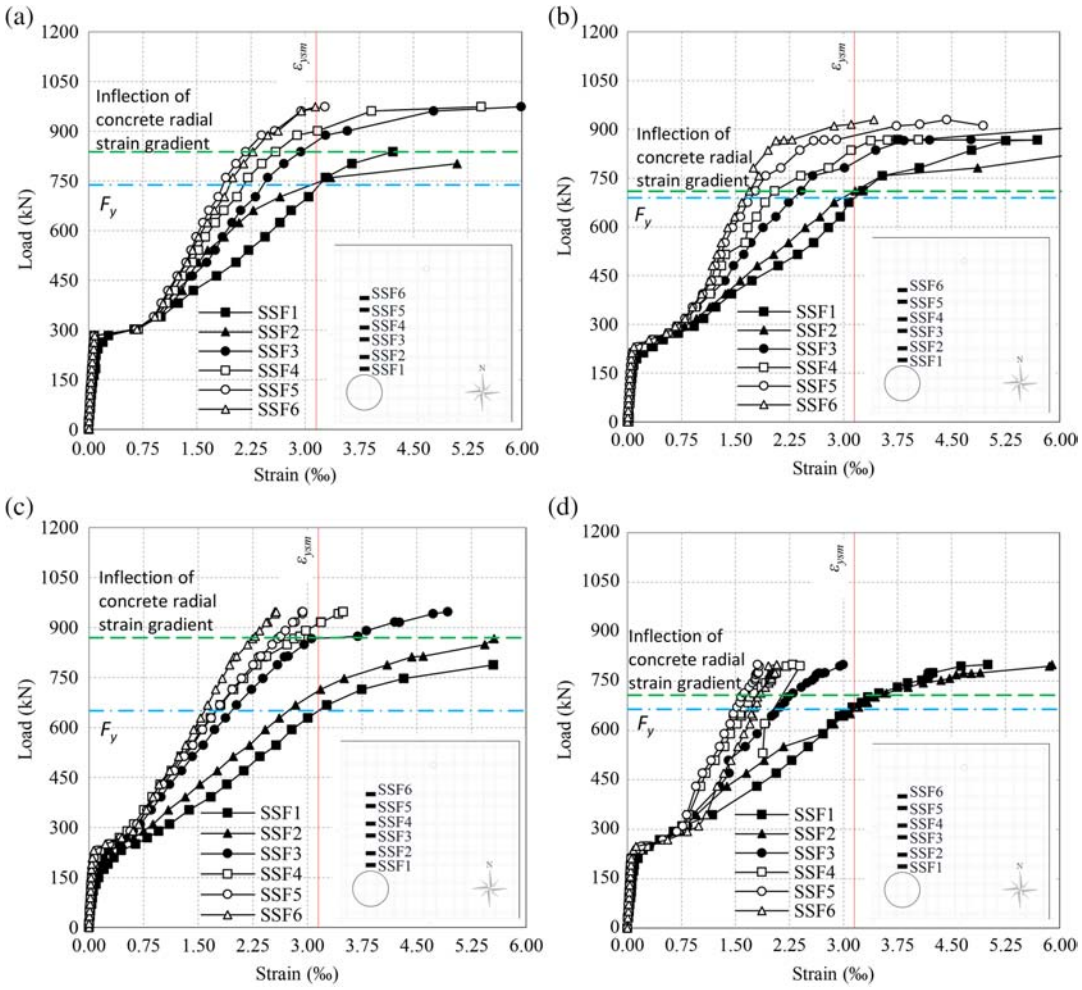

FIGURE 13 Load versus strains in the flexural reinforcement of the slabs: (a) SS, (b) SSP, (c) BD, and (d) BDP. BD, *BubbleDeck* slab; SS, solid slab

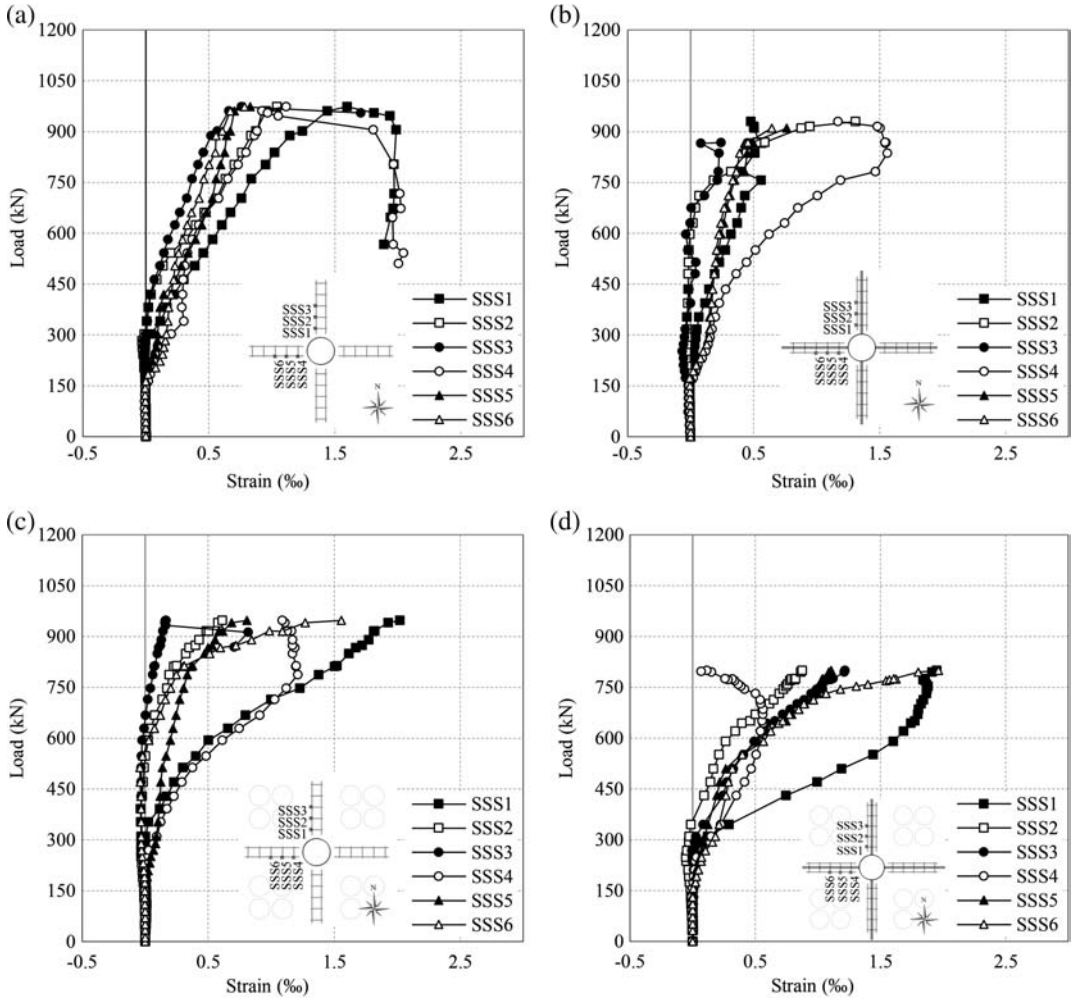

FIGURE 14 Load versus strains in the punching reinforcement of the slabs: (a) SS, (b) SSP, (c) BD, and (d) BDP. BD, *BubbleDeck* slab; SS, solid slab

TABLE 4 Ductility performance of the tested slabs

Slab	Load at yield initiation, F_y (kN)	Average displacement At yield initiation, δ_y (mm)	At maximum load, δ_p (mm)	Ductility index $\mu = \delta_p/\delta_y$
SS	728	9.7	17.1	1.76
SSP	689	8.5	22.4	2.65
BD	651	7.8	15.8	2.04
BDP	675	8.4	12.6	1.51

Abbreviations: BD, *BubbleDeck* slab; SS, solid slab.

top flexural reinforcement. The obtained results are shown in the graphics of Figure 13, where it is also represented the yield strain of this reinforcement, as well as the load level when occurred the inflection of the concrete radial strains reported in the previous section (Figure 12). Some of the strain gauges have ended to work properly when the slabs were approaching their failure stage. The strains were very small up to concrete crack initiation, with an abrupt increase at this stage, followed by a stage of strain gradient as smaller as higher was the distance from the monitored point to the column. At a load level corresponding to the first yield initiation occurrence of the flexural reinforcement, F_y, the gradient of strains have again increased significantly up to the stage of slab's failure. At the failure of the SS slabs, all the six monitored bars have yielded (Figure 13a,b), while only four of these bars have yielded in the BD slab (Figure 13c),

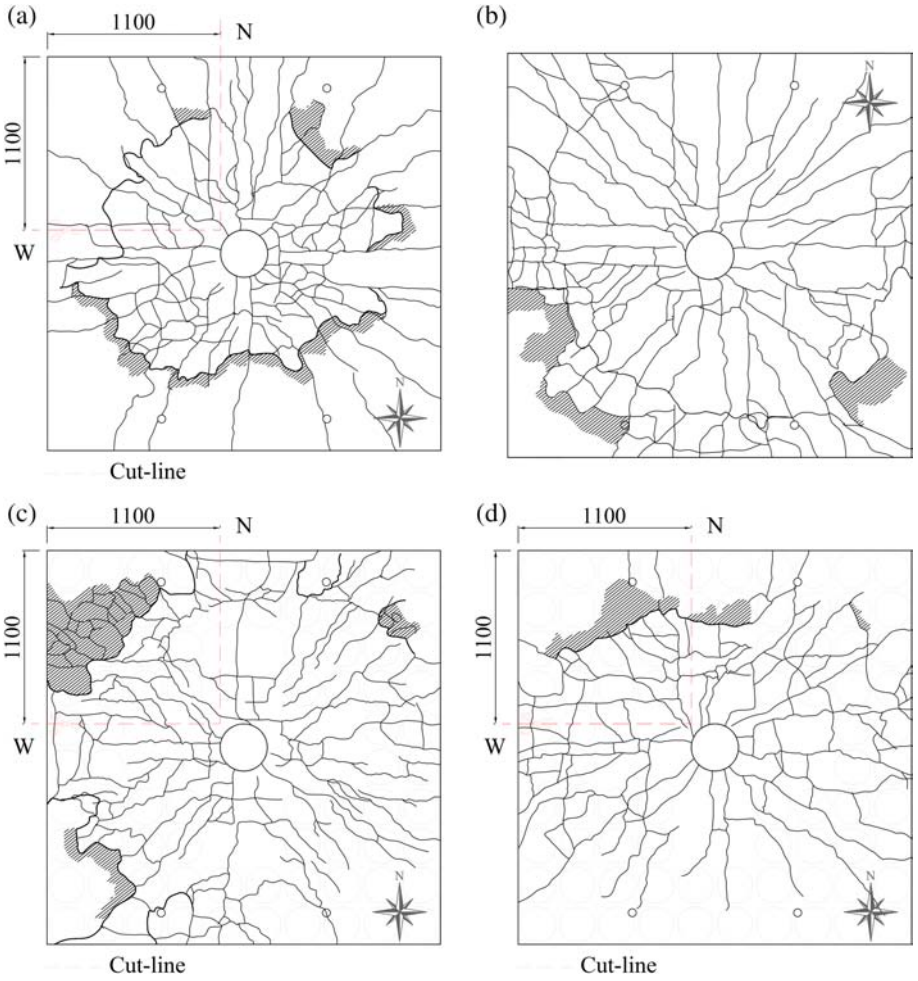

FIGURE 15 Crack pattern in slabs: (a) SS, (b) SSP, (c) BD, and (d) BDP (dimensions in mm). BD, *BubbleDeck* slab; SS, solid slab

and this number was reduced to two bars in the BDP slab (Figure 13d). By applying the yield line theory according to the analytical formulation proposed by Guandalini et al.,[26] and considering for the material properties the average values registered experimentally (provided in Tables 1 and 2), an average value of 1,366 kN with a COV of 0.4% was obtained for the load carrying capacity of the tested slabs assuming they failed in bending. This confirms that, although some flexural bars have yielded, the slabs have failed in punching as will be shown in Section 3.5.

Figure 14 shows the load versus strains in the strain gauges installed on the middle depth of one of the vertical arms of the punching reinforcement, according to the schematic representation in Figure 10b. As expected, the gradient of tensile strains was, in general, as higher as closest to the column the strain gauges were installed. However, none of the monitored stirrups has yielded (the maximum tensile strain was about 2‰, while the yield strain was 3.4‰), which is justified by the punching failure mode observed in all the tested slabs. As expected, the strains were very small up to concrete crack initiation of the slabs, with an appreciable increase after this stage, but not so significant as observed in the strains of the flexural reinforcement (Figure 13).

3.4 | Ductility performance

Table 4 indicates the ductility index, μ, of the tested slabs, being this index obtained as the ratio between the average deflection at peak load (δ_p) and the average deflection at yield initiation of the main flexural reinforcement (δ_y). The force at yield initiation of the main flexural reinforcement (F_y) is also indicated in this table. For the evaluation of the F_y, it was considered the results of Figure 13. According to the obtained results for μ, indicated in Table 4, the ductility performance of the tested slabs, with values ranging from 1.51 to 2.65, was smaller than the value of three recommended elsewhere,[3] which indicates a smaller performance in terms of ductility.

3.5 | Crack pattern at failure stage and configuration of failure surface

The crack pattern was continuously registered during the loading process, and at failure stage of the tested slabs it has the configuration represented in Figure 15. The first observed cracks (of radial type) were registered at about 23% (average value) of the maximum load of the tested slabs. While these radial cracks have progressed, new ones have formed and propagated up to an average load level of 68% of the

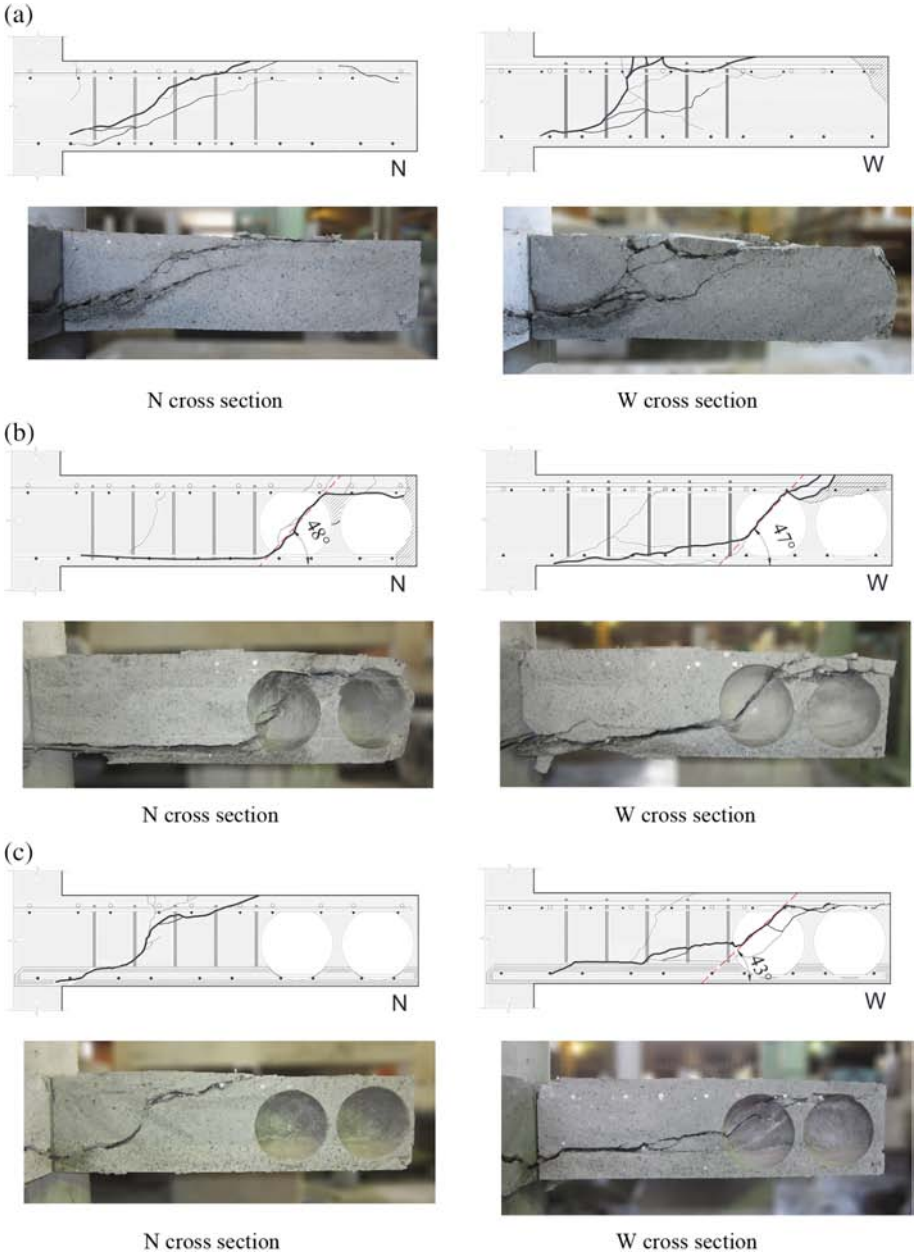

FIGURE 16 Failure surface configuration on the N and W cross sections (Figure 15) of slabs: (a) SS, (b) BD, and (c) BDP. BD, *BubbleDeck* slab; SS, solid slab

maximum load, where the first circumferential cracks become visible. Above this load level, no more radial cracks have arisen, while the opening of the existing radial ones has increased, and new circumferential cracks have formed around the column up to the punching failure occurrence.

To identify the development of the punching shear failure crack and estimate its inclination, the SS, BD, and BDP were sectioned according to the cross sections (N and W) represented in Figure 15. The detected failure surface configuration of these slabs is shown in Figure 16. When crossing the RPHS, the failure surface had an inclination angle varying between 43° and 48° (in agreement with[4]). After crossing the RPHS, the failure surface has propagated almost horizontally along the bottom reinforcement up to the column, while in the top part of the slab it has progressed up to almost the slab's free border.

An unambiguous criterion was not possible to adopt for determining the inclination of the failure surface in the concrete solid zones of the slabs. However, there was a tendency for the failure surface to progress preponderantly in between the second and third stirrups counted from the column's surface (with a relatively high inclination), and to propagate less inclined out of this domain. In the BD slabs, however, there was a clear tendency for the failure surface to cross the first row of RPHS.

4 | CONCLUSIONS

This paper is dedicated to the experimental assessment of the behavior of BD type slab in punching loading conditions, where RPHS are the components disposed in the core

part of this type of slab for decreasing its deadweight. For this purpose, an experimental program composed of four real size RC slabs was carried out, formed by two BD slabs and two solid RC slabs (SS type slabs). The SS slabs are considered the reference slabs, and their difference for the corresponding BD slabs is restricted to the inexistence of the RPHS and girder. In both the BD and SS groups of RC slabs, one of the slabs was built by including a precast RC floor plate. Based on the experimental results, the following main achievements can be pointed out:

1. All the tested slabs failed in punching after the occurrence of yield initiation of the flexural reinforcement. At failure, none of the slabs have experienced inelastic deformation of the transverse reinforcement, and concrete in compression did not crush.
2. When compared to the punching failure capacity of corresponding SS slab, the BD type presented a reduction varying between 4 and 14%, while for the deflection at failure a higher reduction was obtained, ranging from 8 to 44%, having the highest reductions been registered in the slabs with a precast RC floor plates (SSP vs. BDP). In terms of punching capacity, the precast RC floor plates had a more detrimental effect in the BD type slabs (decrease of 15%) than in the SS type slabs (decrease of 5%), but in terms of deflection at failure, a decrease of 20% was registered in the BD, while an increase of 31% was observed in the SS. Considering the relatively small number of tests carried out, nonreliable conclusion can be proposed in this regard, but the authors are working in advanced numerical simulations in order to derive consistent knowledge that can be capable of indicating the influence of the precast RC floor plate in the punching capacity and deformability at failure of SS and BD type slabs.
3. Assuming the ductility index (μ) as the ratio between the slab's deflection at peak load and the deflection at yield initiation of the flexural reinforcement, a μ varying between 1.51 and 2.65 was obtained, which is a relatively small value (some bibliography has recommended a minimum of three for the μ in BD type RC slabs).
4. In the BD type, RC slabs the failure surface presented a tendency to propagate through the RPHS, at an inclination angle of about 45°. This crack has then progressed almost horizontally along the bottom reinforcement up to the column, while in the opposite direction has propagated almost horizontally along the top reinforcement toward the border of the BD slab.

The second part of this publication, in preparation, is devoted to advanced numerical simulations with a software based on the finite element method that includes a 3D concrete crack constitutive model capable of capturing the three fracture modes (opening, sliding, and tearing) occurring in a punching failure mode. After the demonstration of the adequate predictive performance of this constitutive model, using for this purpose the relevant results of the tested slabs prototypes, parametric studies will be performed for calibrating the influence of the parameters of the design guideline to be proposed for the prediction of the punching capacity of BD type slabs.

ACKNOWLEDGMENTS

The authors acknowledge the financial support provided by CAPES (PDSE program/Process number 88881.134825/2016-01) and *BubbleDeck* Brazil. The first author acknowledges, in particular, the support given by the Federal Institute of Brasilia. The authors also acknowledge the support provided by the project ICoSyTec, POCI-01-0145-FEDER-027990, financed by the FCT (Portuguese Foundation for Science and Technology) and co-funded by FEDER through Operational Competitiveness and Internationalization Programme (POCI).

ORCID

Joaquim A. O. Barros https://orcid.org/0000-0003-1528-757X
Guilherme S. S. A. Melo https://orcid.org/0000-0001-9417-9010

REFERENCES

1. Bawens PE. Bending strength and deflection behaviour—Report from the Eindhoven University of Technology. TU Eindhoven. 1999; 71–72.
2. Held MS. Untersuchung an BubbleDeck Modulen—Report from the Technical University of Darmstadt. Darmstadt: Technical University of Darmstadt, 2002.
3. Hashemi SS, Sadeghi K, Vaghefi M, Siadat SA. Evaluation of ductility of RC structures constructed with bubble deck system. Int J Civil Eng. 2018;16(5):513–526. https://doi.org/10.1007/s40999-017-0158-y.
4. Held MS, Pfeffer K. Punching behavior of biaxial hollow slabs. Cem Concr Compos. 2002;24(6):551–556. https://doi.org/10.1016/S0958-9465(01)00071-3.
5. Bubbledeck UK. BubbleDeck voided flat slab solutions—Technical Manual & Documents. BubbleDeck UK head office, Jersey. 2008 [cited [Accessed 2018 Dec 15] Available from http://www.bubbledeck-uk.com/pdf/2-BDTechManualv1a.pdf.
6. Gardner NJ, Huh J, Chung L. Lessons from the Sampoong department store collapse. Cem Concr Compos. 2002;24(6):523–529. https://doi.org/10.1016/S0958-9465(01)00068-3.
7. Valivonis J, Skuturna T, Daugevičius M, Šneideris A. Punching shear strength of reinforced concrete slabs with plastic void formers. Constr Build Mater. 2017;145:518–527. https://doi.org/10.1016/j.conbuildmat.2017.04.057.

8. Ceballos, MA. Experimental analysis of punching shear in BubbleDeck slabs with shear reinforcement [Master's thesis]. University of Brasilia; 2017. Retrieved from http://repositorio.unb.br/handle/10482/24276 (in Portuguese).
9. Silva R, Faria DMV, Ramos AP, Inácio M. A physical approach for considering how anchorage head size influences the punching capacity of slabs strengthened with vertical steel bolts. Struct Concr. 2013;14(4):389–400. https://doi.org/10.1002/suco.201200051.
10. Pérez Caldentey A, Padilla Lavaselli P, Corres Peiretti H, Ariñez Fernández F. Influence of stirrup detailing on punching shear strength of flat slabs. Eng Struct. 2013;49:855–865. https://doi.org/10.1016/J.ENGSTRUCT.2012.12.032.
11. Isufi B, Pinho Ramos A, Lúcio V. Reversed horizontal cyclic loading tests of flat slab specimens with studs as shear reinforcement. Struct Concr. 2019;20(1):330–347. https://doi.org/10.1002/suco.201800128.
12. Teixeira MDE, Barros JAO, Cunha VMCF, Moraes Neto BN, Ventura Gouveia A. Numerical simulation of the punching shear behavior of self-compacting fibre reinforced flat slabs. Constr Build Mater. 2015;74:25–36. https://doi.org/10.1016/j.conbuildmat.2014.10.003.
13. Gouveia ND, Lapi M, Orlando M, Faria DMV, Ramos AMP. Experimental and theoretical evaluation of punching strength of steel fiber reinforced concrete slabs. Struct Concr. 2018;19(1):217–229. https://doi.org/10.1002/suco.201700136.
14. Abdalla KM, Alshegeir A, Chen WF. Analysis and design of mushroom slabs with a strut-tie model. Comput Struct. 1996;58(2):429–434. https://doi.org/10.1016/0045-7949(95)00135-4.
15. Aldejohann M. Zum Querkrafttragverhalten von Hohlkörperdecken mit zweiachsiger Lastabtragung [Master's thesis]. Universität Duisburg-Essen; 2008. Available from https://d-nb.info/990780449/34
16. Valivonis J, Jonaitis B, Zavalis R, Skuturna T, Šneideris A. Flexural capacity and stiffness of monolithic biaxial hollow slabs. J Civ Eng Manag. 2014;20(5):693–701. https://doi.org/10.3846/13923730.2014.917122.
17. Bindea M, Moldovan D, Kiss Z. Flat slabs with spherical voids. Part I: Prescriptions for flexural and shear design Rezumat. Acta Technica Napocensis. 2013;56(1):67–73.
18. Brazilian Association of Technical Standards. NBR 5739—Concrete—Compression test of cylindric specimens—Method of test 2007 (in Portuguese). Rio de Janeiro, Brazil: ABNT.
19. Brazilian Association of Technical Standards. NBR 7222—Mortar and concrete—Determination of the tensile strength of cylindrical specimens submitted to diametrical compression—Method of test 2011 (in Portuguese). Rio de Janeiro, Brazil: ABNT.
20. Brazilian Association of Technical Standards. NBR 8522—Concrete—Determination of the elasticity modulus in compression, 2008 (in Portuguese). Rio de Janeiro, Brazil: ABNT.
21. Brazilian Association of Technical Standards. NBR 5738—Concrete. Test specimens. Molding 2015 (in Portuguese). Rio de Janeiro, Brazil: ABNT.
22. Brazilian Association of Technical Standards. NBR 14931—Execution of concrete structures—Procedure 2004 (in Portuguese). Rio de Janeiro, Brazil: ABNT.
23. Brazilian Association of Technical Standards. NBR ISO 6892—Metallic materials—Tensile testing at ambient temperature 2013 (in Portuguese). Rio de Janeiro, Brazil: ABNT.
24. Barros JAO, Moraes Neto BN, Melo GSSA, Frazão CMV. Assessment of the effectiveness of steel fibre reinforcement for the punching resistance of flat slabs by experimental research and design approach. Compos Part B Eng. 2015;78:8–25. https://doi.org/10.1016/j.compositesb.2015.03.050.
25. Muttoni A. Punching shear strength of reinforced concrete slabs without transverse reinforcement. ACI Struct J. 2008;105(4):440–450. https://doi.org/10.14359/19858.
26. Guandalini S, Burdet O, Muttoni A. Punching tests of slabs with low reinforcement ratios. ACI Struct J. 2009;106(1):87–95. https://doi.org/10.14359/56287.

AUTHOR BIOGRAPHIES

Wanderley G. Nicácio, PhD from the University of Brasilia -UnB
Faculty of Technology, Department of Civil Engineering,
Campus Brasília, SG12, 70910-900 Brasília, Brazil
Email: wanderley.nicacio@gmail.com

Joaquim A. O. Barros, Full Professor
ISISE, Institute of Science and Innovation for Bio-Sustainability (IB-S)
Department of Civil Engineering, University of Minho
4800-058 Guimarães, Portugal
Email: barros@civil.uminho.pt

Guilherme S. S. A. Melo, Full Professor
University of Brasilia-UnB
Faculty of Technology, Department of Civil Engineering
Campus Brasília, 70910-900 Brasília, Brazil
Email: melog@unb.br

How to cite this article: Nicácio WG, Barros JAO, Melo GSSA. Punching behavior of BubbleDeck type reinforced concrete slabs. *Structural Concrete*. 2019; 1–16. https://doi.org/10.1002/suco.201900176